

# Assessment of Myocardial Viability Using $^{123}\text{I}$ -Labeled Iodophenylpentadecanoic Acid at Sustained Low Flow or After Acute Infarction and Reperfusion

Joo Y. Yang, Mirta Ruiz, Dennis A. Calnon, Denny D. Watson, George A. Beller and David K. Glover

*Experimental Cardiology Laboratory, Cardiovascular Division, Department of Medicine, University of Virginia Health Sciences Center, Charlottesville, Virginia*

$^{123}\text{I}$ -labeled iodophenylpentadecanoic acid (IPPA) is a synthetic fatty acid that may be useful for determination of myocardial viability. We investigated the uptake and clearance kinetics of this tracer in canine models of ischemia and infarction. **Methods:** In protocol 1, 185 MBq (5 mCi)  $^{123}\text{I}$ -IPPA were injected intravenously in 19 dogs with 50% left anterior descending artery (LAD) flow reduction. In 9 dogs,  $^{201}\text{Tl}$  was coinjected. In protocol 2, 5 dogs underwent LAD occlusion for 3 h, and  $^{123}\text{I}$ -IPPA was injected 60 min after reperfusion. All dogs had flow measured by microspheres, regional systolic thickening by ultrasonic crystals and measurements of postmortem risk area and infarct size. Tracer activities were quantified by gamma well counting and by serial imaging. **Results:** In protocol 1 dogs with sustained low flow (50%  $\pm$  4%) and absence of systolic thickening ( $-3.2\% \pm 1\%$ ),  $^{123}\text{I}$ -IPPA defect magnitude (LAD/left circumflex artery [LCX] count ratios) decreased from  $0.65 \pm 0.02$  to  $0.74 \pm 0.02$  at 30 min and to  $0.84 \pm 0.03$  at 2 h ( $P < 0.01$ ), indicative of rest redistribution. Final transmural  $^{123}\text{I}$ -IPPA LAD/LCX activity ratio ( $0.99 \pm 0.05$ ) was significantly greater than the flow ratio ( $0.53 \pm 0.04$ ) at injection, confirming complete rest redistribution. The final  $^{123}\text{I}$ -IPPA activity ratio was significantly greater than the  $^{201}\text{Tl}$  ratio over the 2-h period ( $P < 0.01$ ). In protocol 2 dogs that underwent 3 h of total LAD occlusion and reflow (infarct size =  $51\% \pm 13\%$  of risk area), viability was overestimated with  $^{123}\text{I}$ -IPPA, because uptake averaged 64% of normal in the central necrotic region, where flow averaged  $<10\%$  of normal. **Conclusion:** These findings suggest that serial  $^{123}\text{I}$ -IPPA imaging may be useful for assessing myocardial viability under conditions of sustained low flow and myocardial asynergy, such as appears to exist in patients with chronic coronary artery disease and depressed left ventricular function. In contrast,  $^{123}\text{I}$ -IPPA given early after reperfusion following prolonged coronary occlusion overestimates the degree of viability and therefore may not provide useful information pertaining to the degree of myocardial salvage after reflow in the setting of acute myocardial infarction.

**Key Words:** myocardial viability; radionuclide imaging; fatty acids;  $^{201}\text{Tl}$ ; myocardial ischemia; myocardial infarction

**J Nucl Med 1999; 40:821-828**

**A**ccurate assessment of myocardial viability in patients with chronic coronary artery disease (CAD) or acute myocardial infarction is essential for determining which patients will benefit most from coronary revascularization. Rest  $^{201}\text{Tl}$  redistribution imaging and PET imaging of perfusion and fluorodeoxyglucose (FDG) uptake are being widely used for the assessment of myocardial viability in patients with chronic CAD.

In addition to FDG,  $^{11}\text{C}$ -palmitate has been used clinically for assessing myocardial viability with PET imaging (1,2). While FDG uptake reflects myocardial glucose intracellular transport and phosphorylation,  $^{11}\text{C}$ -palmitate uptake and clearance reflects fatty acid metabolism. The widespread use of positron-emitting tracers of myocardial metabolism for the assessment of myocardial viability has been hindered by the relatively short half-life of the PET tracers, which requires an on-site cyclotron, and by the limited number of PET scanners.  $^{123}\text{I}$ -labeled iodophenylpentadecanoic acid (IPPA) is a synthetic fatty acid with myocardial kinetics that are similar to  $^{11}\text{C}$ -palmitate (3-5). Unlike  $^{11}\text{C}$ -palmitate, the 159 keV  $^{123}\text{I}$  photopeak is optimal for gamma camera imaging, and its 13-h half-life obviates an on-site cyclotron. A clinical study comparing  $^{123}\text{I}$ -IPPA with  $^{201}\text{Tl}$  in patients with resting left ventricular (LV) dysfunction demonstrated a greater degree of defect reversibility with  $^{123}\text{I}$ -IPPA than with  $^{201}\text{Tl}$ , particularly in myocardial segments with mild-to-moderate fixed  $^{201}\text{Tl}$  defects (6). In addition,  $^{123}\text{I}$ -IPPA defect reversibility was predictive of recovery of LV dysfunction after revascularization.

In this study, we sought to define the kinetics of  $^{123}\text{I}$ -IPPA in canine models of sustained low flow or prolonged coronary occlusion and reperfusion to determine the poten-

Received May 27, 1998; revision accepted Sep. 15, 1998.

For correspondence or reprints contact: David K. Glover, ME, Cardiovascular Division, Department of Medicine, Box 500, University of Virginia Health Sciences Center, Charlottesville, VA 22908.

tial suitability of  $^{123}\text{I}$ -IPPA imaging for the assessment of myocardial viability in patients with chronic CAD and severe resting LV dysfunction and in patients with acute infarction. Specifically, we compared the myocardial uptake and redistribution kinetics of  $^{123}\text{I}$ -IPPA with  $^{201}\text{Tl}$  in dogs with sustained low flow and in dogs that underwent 3 h of coronary occlusion and reperfusion.

## MATERIALS AND METHODS

### Surgical Preparation

Twenty-four mongrel dogs that had been previously fasted overnight were anesthetized with sodium pentobarbital (30 mg/kg), intubated and ventilated on a respirator (Model 603; Harvard Apparatus, S. Natick, MA). The left femoral vein was cannulated with an 8F polyethylene catheter for administration of fluids, medications and radionuclides. Both femoral arteries were isolated and cannulated with 8F polyethylene catheters for blood pressure monitoring, collection of arterial blood samples and microsphere reference blood withdrawal. The ventilator was adjusted and bicarbonate administered to maintain blood gases within the normal physiologic range.

A thoracotomy was performed at the fifth intercostal space, and the heart was suspended in a pericardial cradle. A flare-tipped polyethylene catheter was inserted into the left atrial appendage for pressure measurement and injection of microspheres. Proximal segments (1.5 cm) from both the left anterior descending artery (LAD) and the left circumflex artery (LCX) were dissected free of the epicardium. Ultrasonic flow probes (Model T201; Transonic Systems Inc., Ithaca, NY) were placed on the LAD and LCX coronary arteries. A snare ligature was then placed proximal to the LAD probe. Two Doppler sonomicrometer crystals (Crystal Biotech, Holliston, MA) were sutured to the epicardial surface of the heart in the regions supplied by the LAD and LCX, respectively, to measure regional wall thickening. An 8-channel stripchart recorder (Model 7758A; Hewlett-Packard Co., Lexington, MA) was used to monitor lead II of the electrocardiogram, arterial and left atrial pressures, ultrasonic LAD and LCX flows and regional LAD and LCX systolic wall thickening. All experiments were performed with the approval of the University of Virginia Animal Research Committee, in compliance with the position of the American Heart Association on use of research animals.

### Experimental Protocols

*Protocol 1: Myocardial and Blood Kinetics of  $^{123}\text{I}$ -IPPA Under Conditions of Sustained Low Flow and Regional Dysfunction.* After a 20-min baseline period, the snare ligature was adjusted in 19 open-chest dogs to reduce LAD flow by 50% as measured by the ultrasonic flow probe. After 30–60 min, 185 MBq (5 mCi)  $^{123}\text{I}$ -IPPA (Nordion International, Inc., Vancouver, BC) was injected intravenously, and images were obtained at 2, 4, 6, 8, 10, 20, 30, 60 and 120 min postinjection. In 7 of the 19 dogs, 1.0 mL arterial blood samples were simultaneously withdrawn into preweighed tubes at 30 s, and at 1, 1.5, 2, 4, 6, 8, 10, 20, 30, 60 and 120 min after  $^{123}\text{I}$ -IPPA injection. In addition, in 9 dogs 37 MBq (1 mCi)  $^{201}\text{Tl}$  was also administered approximately 10 min before the  $^{123}\text{I}$ -IPPA injection, and an initial set of  $^{201}\text{Tl}$  images was acquired. Radiolabeled microspheres were injected at baseline, with  $^{123}\text{I}$ -IPPA injection, and at the end of the protocol for the measurement of regional myocardial flow at these time points. Dogs receiving

$^{201}\text{Tl}$  were also given microspheres at the time of injection. The microspheres used in these experiments were either  $^{113}\text{Sn}$ ,  $^{103}\text{Ru}$ ,  $^{95}\text{Nb}$  or  $^{46}\text{Sc}$ . At the end of the protocol, the LAD was briefly occluded and monastral blue dye was injected into the left atrial catheter to delineate the anatomic risk area. The dogs were then immediately killed with a lethal dose of sodium pentobarbital.

*Protocol 2: Myocardial Kinetics of  $^{123}\text{I}$ -IPPA when Administered After Reperfusion Following a 3-Hour LAD Occlusion.* After baseline measurements, the LAD and visible feeder collaterals from the LCX in 5 dogs were totally occluded for 3 h.  $^{123}\text{I}$ -IPPA was injected 60 min after reperfusion, and serial images were acquired over the next 2 h. The LAD was then briefly reoccluded, and monastral blue dye was injected into the left atrial catheter as previously described. The dogs were then killed.

### Postmortem Analysis

At the end of each protocol, the hearts were immediately excised and sliced evenly from apex to base into four segments. The LV and septum were then separated from the remainder of the heart, and photographed. Each slice was then carefully traced on acetate sheets to define the endocardial and epicardial borders and the area at risk. Slices were subsequently incubated in 1% phosphate-buffered triphenyl tetrazolium chloride (TTC) solution at 37°C for 10 min to define infarct size, then rephotographed and retraced on the same acetate sheets. With a digital planimeter program, risk area and infarct area were determined.

### Image Acquisition and Quantification of Defect Count Ratio

All images were acquired in the left lateral projection with a standard nuclear medicine gamma camera and computer (Technicare 420; Ohio Nuclear, Solon, OH), using an all-purpose, low-to-medium energy collimator with a 20% window centered around the photopeak of  $^{123}\text{I}$ . In protocol 1 studies with  $^{201}\text{Tl}$  imaging, a 25% window centered around the photopeak of  $^{201}\text{Tl}$  was also used. A lead shield was placed over the abdomen to reduce liver and splanchnic activity.

Image quantification and background subtraction were performed on a nuclear medicine computer (SMV America, Twinsburg, OH). The background subtraction algorithm has previously been described (7). No thresholding or filtering was applied to the images. To quantify  $^{123}\text{I}$  or  $^{201}\text{Tl}$  activities on images, regions of interest (ROIs) were drawn on the defect area of the anteroseptal LV wall and on the normally perfused posterior wall of each image. The ROIs were drawn to encompass as large an amount of the region in question without including border areas. The serial  $^{123}\text{I}$ -IPPA images were aligned, and average counts were taken from the same regions on each image. The in vivo defect count ratio was computed by dividing the average counts per pixel in the ischemic region by the average counts per pixel in the nonischemic region.

In protocol 2, an additional image was obtained by placing the ex vivo heart slices directly on the collimator of the gamma camera and imaging for maximal count time by using  $^{123}\text{I}$  window settings.

### Determination of Regional Myocardial Blood Flow Using Radioactive Microspheres and Quantification of Tracer Uptake

The technique used in our laboratory for quantification of regional myocardial blood flow using radioactive microspheres has been previously described (8). A dose of spheres (2–5 million; mean diameter 11  $\mu\text{m}$ ) was suspended in 3 mL normal saline and

0.01% Tween 80. Uniform mixing was accomplished initially by mechanical agitation (Vortex Genie mixer; Scientific Products, Bohemia, NY), followed by hand agitation between two syringes attached with a three-way stopcock. The microspheres were administered over 15 s into the left atrium. For flow determination, paired arterial reference samples were obtained by continuous withdrawal (Model 944; Harvard Apparatus) over 130 s, beginning 10 s before the injection of each set of spheres. Each of the four myocardial slices was divided into six transmural sections that were further subdivided into epicardial, midwall and endocardial segments, resulting in a total of 72 myocardial segments for each dog. The myocardial segments and arterial blood samples were counted for  $^{123}\text{I}$ -IPPA activities in a gamma well scintillation counter (MINAXI 5550; Packard Instruments, Downers Grove, IL) within 24 h by using a window setting of 90–230 keV. After 24–48 h, when the  $^{123}\text{I}$ -IPPA activity had decayed, the myocardial and blood samples were counted for  $^{201}\text{Tl}$  activity by using a window setting of 50–100 keV. When  $^{201}\text{Tl}$  activity was negligible, 3 wk later, the myocardial samples were counted a third time for microsphere regional blood flow determination. The microsphere window settings were:  $^{113}\text{Sn}$ , 340–440 keV;  $^{103}\text{Ru}$ , 450–550 keV;  $^{95}\text{Nb}$ , 640–840 keV; and  $^{46}\text{Sc}$ , 842–1300 keV. Tissue counts were corrected for background, decay and isotope spillover and regional myocardial blood flow calculated using computer software developed for this purpose (PCGERDA, Scientific Computing Solutions, LLC, Charlottesville, VA). The transmural regional flow values for a specific sample were derived from the weighted average of epicardial, midwall and endocardial values for that sample.

### Statistical Analysis

Computations were performed with Systat software (SPSS, Inc., Chicago, IL). Results were expressed as mean values  $\pm$  1 SEM. Differences over time were determined with repeated measures of analysis of variance with appropriate posthoc comparisons. Single pair comparisons were made with a paired *t* test. Differences were considered significant at a *P* value of  $< 0.05$  (2-tailed).

## RESULTS

### Protocol 1: Myocardial and Blood Kinetics of $^{123}\text{I}$ -IPPA Under Conditions of Sustained Low Flow and Regional Dysfunction

**Hemodynamics.** Hemodynamic parameters of heart rate, systemic arterial pressure, left atrial pressure, LAD and LCX flows measured at baseline, after setting the LAD stenosis and at the end of the protocol, are summarized in Table 1. As shown, the dogs were hemodynamically stable over the experimental time course, although there was a slight tendency for heart rate and arterial pressure to fall over time. Despite these changes, LCX flow remained constant. In the LAD, imposition of the coronary stenosis resulted in a decrease in flow to approximately 50% of the baseline value, where it remained stable thereafter.

**Wall Thickening.** After setting the LAD stenosis, regional LAD thickening fell from  $24\% \pm 2\%$  to  $-3.2\% \pm 1\%$  ( $P < 0.01$ ) and remained dyskinetic over the following 2 h ( $-2.5\% \pm 1\%$ ). Baseline LCX thickening was  $21\% \pm 2\%$ , and there was a slight compensatory increase in thickening to  $24\% \pm 2\%$  after setting the LAD stenosis. This change

**TABLE 1**  
Hemodynamic Parameters for Protocol 1 Dogs

	Base	Stenosis IPPA	End
HR (bpm)	141 $\pm$ 2	137 $\pm$ 4	128 $\pm$ 3
AP (mm Hg)	117 $\pm$ 3	113 $\pm$ 2	109 $\pm$ 2
LAP (mm Hg)	9 $\pm$ 0	10 $\pm$ 1	11 $\pm$ 0
LAD flow (mL/min)	27 $\pm$ 2	11 $\pm$ 1*	11 $\pm$ 1*
LCX flow (mL/min)	40 $\pm$ 3	39 $\pm$ 3	40 $\pm$ 4

\**P* < 0.01 vs. baseline value.

Base = baseline; IPPA = iodophenylpentadecanoic acid; HR = heart rate; AP = arterial pressure; LAP = left atrial pressure; LAD = left anterior descending artery; LCX = left circumflex artery.

Values expressed as mean  $\pm$  SEM.

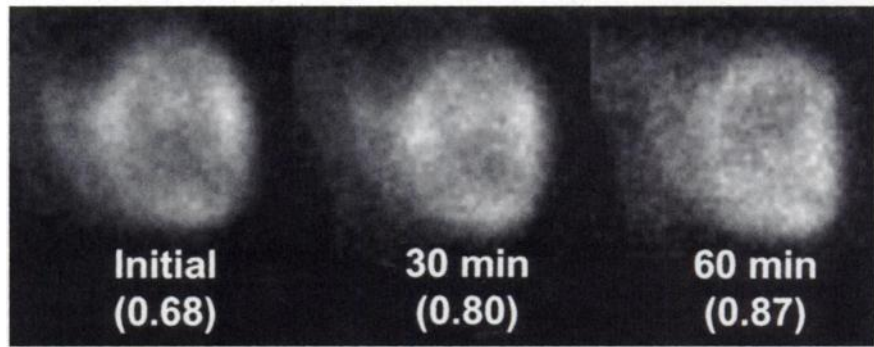
did not reach statistical significance. Over the 2-h redistribution period, there was no further change in LCX thickening.

**Anatomic Risk Area and Infarct Size.** The mean anatomic risk area as determined by monastral blue dye was  $31.1\% \pm 1.2\%$  of the LV. The infarct size was  $2.0\% \pm 1.0\%$  of the LV and  $5.8\% \pm 2.4\%$  of the risk area. In 12 of the 19 dogs, the infarct size averaged less than 1% of the LV, with 9 of the 19 hearts showing no evidence of myocardial infarction.

**$^{123}\text{I}$ -IPPA Blood Clearance.**  $^{123}\text{I}$ -IPPA activities from the arterial blood samples that were collected in 7 dogs were expressed as a percentage of the initial activity at 30 s.  $^{123}\text{I}$ -IPPA blood activity fell rapidly to  $40\% \pm 5\%$  of the initial activity in the first 2 min. By 10 min,  $^{123}\text{I}$ -IPPA blood activity had fallen to  $9\% \pm 1\%$  of initial activity and then remained at that level over the next 110 min.

**Image Count Ratios and Clearance Kinetics of  $^{123}\text{I}$ -IPPA.** Figure 1 shows a representative set of images from a dog in protocol 1. As shown, there was a prominent anteroseptal perfusion defect present initially (LAD/LCX count ratio = 0.68) that had nearly resolved (0.80) at 30 min. By 60 min, the count ratio was 0.87. The mean defect count ratios for the entire group of dogs are depicted in the bar graph shown in Figure 2. The  $^{201}\text{Tl}$  mean defect count ratio from the 9 dogs receiving  $^{201}\text{Tl}$  in addition to  $^{123}\text{I}$ -IPPA is shown for comparison (solid bar). As can be seen, the  $^{201}\text{Tl}$  and initial  $^{123}\text{I}$ -IPPA image count ratios were similar ( $0.64 \pm 0.04$  versus  $0.65 \pm 0.02$ ). The  $^{123}\text{I}$ -IPPA image count ratio progressively increased (decreasing defect magnitude) to  $0.74 \pm 0.02$ ,  $0.78 \pm 0.02$  and  $0.84 \pm 0.03$  at 30, 60 and 120 min, respectively ( $P < 0.01$  versus initial). The  $^{123}\text{I}$ -IPPA activities (counts/pixel/min) obtained from the LAD and LCX ROIs drawn on the serial background subtracted in vivo images are plotted in Figure 3. Peak  $^{123}\text{I}$ -IPPA uptake occurred at the 6-min time point in both the LAD and LCX regions. As can be seen in Figure 3, myocardial clearance of  $^{123}\text{I}$ -IPPA was biphasic, with a rapid early phase occurring during the initial 20–30 min, followed by a slower late phase. Note that the rapid early clearance phase was significantly faster in the normal LCX, compared with the sustained low-flow LAD region.

**FIGURE 1.** Representative in vivo images acquired at 5, 30 and 60 min in protocol 1 dog with sustained low flow. Numbers in parentheses below each image are defect count ratios.  $^{123}\text{I}$ -IPPA redistribution on serial imaging was rapid with substantial amount occurring in first 30 min postinjection.



**Regional Myocardial Blood Flow and  $^{123}\text{I}$ -IPPA and  $^{201}\text{Tl}$  Activities.** The transmural regional myocardial blood flow ratio (LAD/LCX) at the time when  $^{123}\text{I}$ -IPPA was injected is shown on the left in Figure 4 (striped bar). For comparison purposes, the mean  $^{201}\text{Tl}$  flow ratio obtained from the 9 dogs receiving  $^{201}\text{Tl}$  in addition to  $^{123}\text{I}$ -IPPA is also shown on the left (solid bar). There was no difference in the regional myocardial blood flow ratios at the times when either  $^{123}\text{I}$ -IPPA or  $^{201}\text{Tl}$  was injected ( $0.53 \pm 0.04$  versus  $0.50 \pm 0.05$ ). The final transmural  $^{123}\text{I}$ -IPPA activity ratio (LAD/LCX; right striped bar) measured by gamma well counting was  $0.99 \pm 0.05$  and was significantly greater than the flow ratio at the time when  $^{123}\text{I}$ -IPPA was injected ( $0.53$ ) ( $P < 0.01$ ). This suggests a normalization of the  $^{123}\text{I}$ -IPPA “defect” over the 2-h  $^{123}\text{I}$ -IPPA postinjection. Similarly, in the dogs receiving  $^{201}\text{Tl}$ , the final  $^{201}\text{Tl}$  activity ratio ( $0.69 \pm 0.05$ ) was significantly greater than the flow ratio at the time when  $^{201}\text{Tl}$  was administered ( $0.50$ ) ( $P < 0.01$ ), indicating rest  $^{201}\text{Tl}$  redistribution.

**Protocol 2: Myocardial Kinetics of  $^{123}\text{I}$ -IPPA When Administered After Reperfusion Following a 3-Hour Total LAD Occlusion**

**Hemodynamics.** The hemodynamic parameters for protocol 2 are summarized in Table 2. Heart rate fell slightly

during the 3-h LAD occlusion but had returned to baseline after 60 min of reperfusion at the time when  $^{123}\text{I}$ -IPPA was injected. Mean arterial pressure also fell during the occlusion and reperfusion periods but was  $109 \pm 5$  mm Hg at the time when  $^{123}\text{I}$ -IPPA was injected. LAD flow fell from 26 to 0 during the 3-h occlusion, ( $P < 0.05$ ). After reperfusion, there was a small reactive hyperemic response, although this change did not reach statistical significance. By 60 min after reperfusion, LAD flow had returned to baseline ( $23 \pm 6$ ). There was no significant change in either left atrial pressure or LCX coronary flow during these experiments.

**Wall Thickening.** Systolic thickening in the LAD territory was  $21\% \pm 3\%$  at baseline and fell to  $-3\% \pm 1\%$  during the 3-h occlusion ( $P < 0.01$ ). After reperfusion, LAD thickening worsened to  $-7\% \pm 2\%$  ( $P < 0.01$  versus occlusion). It remained dyskinetic at the times when  $^{123}\text{I}$ -IPPA was injected ( $-5\% \pm 1\%$ ) and 2 h later ( $-4\% \pm 1\%$ ). Mean LCX thickening was  $19\% \pm 1\%$  at baseline and was unchanged over the experimental time course. LCX thickening was  $19\% \pm 3\%$  after reperfusion when  $^{123}\text{I}$ -IPPA was injected.

**Anatomic Risk Area and Infarct Size.** The anatomic risk area determined by monastral blue dye injection was  $25.5\% \pm 2\%$  of the LV. By TTC stain, there were large infarcts in all 5 dogs. The mean infarct size was  $13.9\% \pm 3\%$  of the LV and

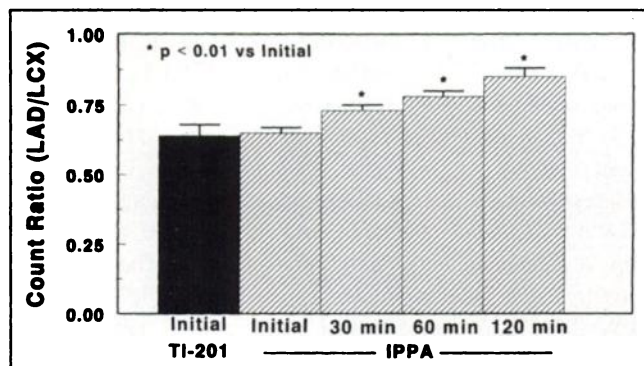


**FIGURE 2.** Bar graph depicting mean count ratios (LAD/LCX) from  $^{123}\text{I}$ -IPPA imaging (striped bars) at 5, 30, 60 and 120 min postinjection in protocol 1 dogs with sustained low flow. Shown for comparison is mean initial count ratio for  $^{201}\text{Tl}$  from 9 dogs injected with  $^{201}\text{Tl}$  plus  $^{123}\text{I}$ -IPPA (black bar). Note that count ratios for  $^{201}\text{Tl}$  and  $^{123}\text{I}$ -IPPA were similar initially, and there was significant, rapid redistribution of  $^{123}\text{I}$ -IPPA over 2 h, despite sustained low flow.

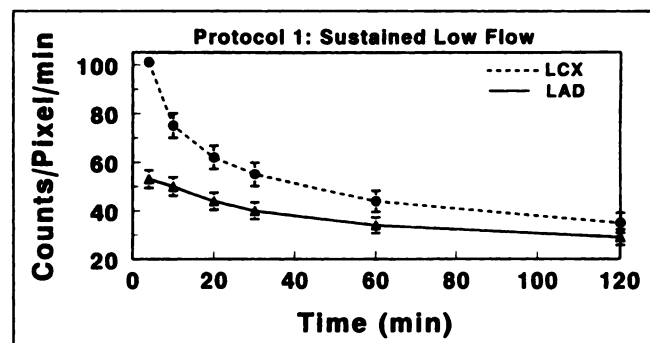


**FIGURE 3.** Time-activity curves obtained from ROIs drawn on serial  $^{123}\text{I}$ -IPPA images from protocol 1 dogs. Dashed line represents myocardial  $^{123}\text{I}$ -IPPA clearance from normal LCX zone, and solid line represents clearance from low-flow LAD zone. Data points on each curve are mean counts/pixel/min at each time point.  $^{123}\text{I}$ -IPPA myocardial clearance was biphasic. Early phase was significantly faster in normal LCX compared with low-flow LAD zone.

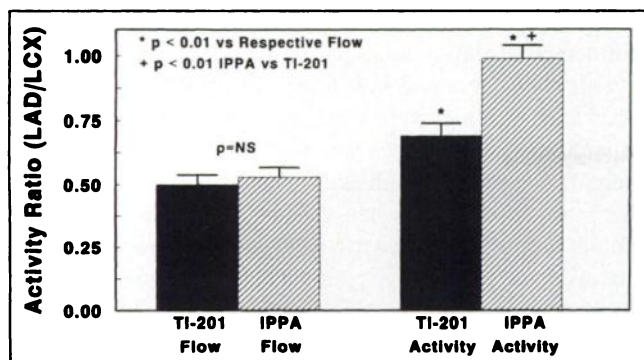


**FIGURE 4.** Bar graph comparing regional myocardial blood flow ratios (LAD/LCX) at times when <sup>201</sup>Tl and <sup>123</sup>I-IPPA were injected (left pair of bars) with final 2-h tracer activity ratios (LAD/LCX) (right pair) as determined by gamma well counting in protocol 1 dogs. Note that flow ratios were identical at times when <sup>201</sup>Tl and <sup>123</sup>I-IPPA were administered. <sup>123</sup>I-IPPA redistribution was nearly complete 2 h later, and there was a significantly greater degree of <sup>123</sup>I-IPPA redistribution compared with <sup>201</sup>Tl.

50.6% ± 12.7% of the myocardial risk area (range 25%–98%).

**Image Count Ratios and Myocardial Clearance Kinetics of <sup>123</sup>I-IPPA in Reperfused Myocardium.** The mean defect count ratios (LAD/LCX) obtained from quantitation of background subtracted in vivo images are shown in Figure 5. As can be seen, there was substantial initial uptake of <sup>123</sup>I-IPPA in the reperfused region, with an initial defect count ratio of 0.63 ± 0.03. By 60 min, the defect count ratio had significantly increased to 0.84 ± 0.08, with a further increase to 0.91 ± 0.07 at 120 min. In Figure 6, the mean <sup>123</sup>I-IPPA activities from the LAD and LCX ROIs (counts/pixel/min) are plotted against time. Note that there was significantly faster myocardial clearance of <sup>123</sup>I-IPPA from the normal, LCX region compared with the reperfused LAD region, particularly in the first 30 min. In the reperfused LAD region, there was also a brief period of rapid clearance between 5 and 15 min. Interestingly, in 1 dog a “hot spot” (area of increased <sup>123</sup>I-IPPA uptake) was observed on the anteroseptal wall in the late (120 min) images. Although hot spots were not observed on the in vivo images of the other 4

dogs in this protocol, hot spots were observed on the ex vivo images in all 5 dogs (Fig. 7). The hot spots were located in the reperfused LAD region on one or both of the two central slices from each heart. Within three of the five hot spots, there were also regions of reduced count density. These reduced count density areas corresponded to infarct regions as determined by TTC staining.

**Regional Myocardial Blood Flow and <sup>123</sup>I-IPPA Uptake.** The mean transmural microsphere flow ratio (LAD/LCX) was 0.86 ± 0.01 at baseline and fell to 0.22 ± 0.02 during the 3-h LAD occlusion. The corresponding endocardial flow ratio during the occlusion was 0.10 ± 0.03. At the time when <sup>123</sup>I-IPPA was injected, 60 min after reperfusion, the transmural flow ratio was 1.03 ± 0.03, indicating complete reflow without significant reactive hyperemia. The final <sup>123</sup>I-IPPA activity ratio (LAD/LCX) (0.82 ± 0.11) was not significantly lower than the reperfusion flow ratio, despite substantial infarction of the reperfused territory. In Figure 8, <sup>123</sup>I-IPPA activities in myocardial segments were grouped according to the severity of their occlusion flow reduction. The activities were expressed as a percentage of uptake in normal segments. As shown, even in segments with the most severe flow reduction during the occlusion period (<10% normal), there was substantial relative uptake and retention of <sup>123</sup>I-IPPA (64%). In addition, in the intermediate flow reduction regions (21%–60% normal), <sup>123</sup>I-IPPA activity exceeded the activity in the normal regions by 20%–25% and was also higher than the flow in each of the corresponding segments.

## DISCUSSION

The experimental data from the two protocols used in this study suggest that <sup>123</sup>I-IPPA imaging for the noninvasive assessment of myocardial viability may present difficulties in differentiating viable but underperfused myocardium (protocol 1) from acutely reperfused but necrotic myocardium (protocol 2). Uptake of the radiolabeled fatty acid in hypoperfused, asynergic myocardium is comparable with delayed <sup>201</sup>Tl uptake that is reflective of viability. Substantial <sup>123</sup>I-IPPA uptake, however, can also be seen in necrotic

**TABLE 2**  
Hemodynamic Parameters for Protocol 2 Dogs

	Base	Occ	Rep	IPPA	End
HR (bpm)	142 ± 7	134 ± 7*	152 ± 11	135 ± 8	134 ± 7*
AP (mm Hg)	124 ± 7	115 ± 9	100 ± 5*	109 ± 5*	113 ± 6
LAP (mm Hg)	10 ± 1	9 ± 1	11 ± 1	11 ± 1	11 ± 1
LAD flow (mL/min)	26 ± 5	0 ± 0*	32 ± 6	23 ± 6	19 ± 5
LCX flow (mL/min)	47 ± 9	38 ± 9	40 ± 6	36 ± 8	37 ± 7

\*P < 0.05 vs. baseline value.

Base = baseline; Occ = occlusion; Rep = reperfusion; IPPA = iodophenylpentadecanoic acid; HR = heart rate; AP = arterial pressure; LAP = left atrial pressure; LAD = left anterior descending artery; LCX = left circumflex artery.

Values expressed as mean ± SEM.

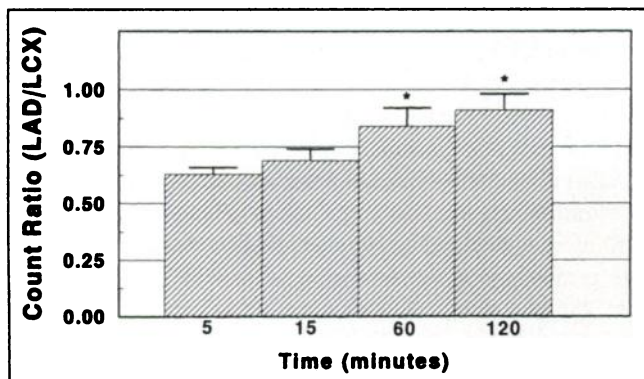


**FIGURE 5.** Bar graph comparing mean defect count ratios (LAD/LCX) over time in protocol 2 dogs that underwent 3 h of occlusion and 1 h of reperfusion before  $^{123}\text{I}$ -IPPA injection. Despite 50% infarction of risk area, there was a substantial amount of  $^{123}\text{I}$ -IPPA uptake at 5 min, with significant redistribution by 60 min.

myocardium in the situation when the tracer is administered soon after reperfusion, preceded by 3 h of coronary occlusion. In this instance, the  $^{123}\text{I}$ -IPPA scan pattern would significantly overestimate myocardial viability. Normalization of  $^{123}\text{I}$ -IPPA uptake in the infarct-reperfusion canine experimental model may merely be secondary to rapid washout of the tracer from normal myocardium with impaired uptake and washout in the infarct zone (Fig. 6).

#### Myocardial and Blood Kinetics of $^{123}\text{I}$ -IPPA Under Conditions of Sustained Low Flow and Regional Dysfunction

Immediately after injection, arterial IPPA blood activity fell rapidly to <10% of initial activity within the first 10 min and remained low over the next 2 h. The rapid blood pool clearance results from the terminal iodophenyl substitution on IPPA that yields iodobenzoic acid as the end product of fatty acid catabolism (3). The iodobenzoic acid and its metabolite hippurate are both rapidly eliminated from the blood pool by the kidneys. This is in contrast to the straight chain fatty acid analogs, such as iodoheptadecanoic acid, in which the end product is free radioiodide that accumulates in the blood pool and degrades image quality (9).

In this protocol, in which LAD flow was reduced by approximately 50%, causing lack of systolic thickening but virtually no infarction, significant differences in myocardial  $^{123}\text{I}$ -IPPA clearance over 2 h were observed. As has previously been demonstrated with both palmitic acid and  $^{123}\text{I}$ -IPPA (10,11), myocardial  $^{123}\text{I}$ -IPPA clearance from normal myocardium was biphasic. The early rapid clearance phase results from  $^{123}\text{I}$ -IPPA metabolism by  $\beta$  oxidation, whereas the slower clearance phase represents the turnover of the  $^{123}\text{I}$ -IPPA incorporated in the triglyceride and phospholipid pools (4,5). After reaching peak myocardial uptake, the mechanism by which  $^{123}\text{I}$ -IPPA image defects resolved over time was due to a more rapid early phase clearance of the tracer from the normally perfused LCX zone compared with the low-flow LAD zone (see Fig. 3).

Interestingly, both  $^{201}\text{Tl}$  and  $^{123}\text{I}$ -IPPA exhibited significant defect resolution more than 2 h after injection in these animals with sustained low flow, but by different mechanisms. By gamma well counting, the LAD/LCX tissue activity ratios for  $^{201}\text{Tl}$  ( $0.69 \pm 0.05$ ) and  $^{123}\text{I}$ -IPPA ( $0.99 \pm 0.05$ ) after 2 h were significantly higher than the LAD/LCX flow ratios at the time when the two tracers were injected. The amount of  $^{201}\text{Tl}$  redistribution over 2 h was similar to what we have previously reported in canine models, with a 50% sustained flow reduction (12,13). Our findings in this sustained low flow model are consistent with the observations made in the clinical  $^{123}\text{I}$ -IPPA studies. Iskandrian et al. (6) studied 21 patients with resting LV dysfunction (ejection fraction [EF] =  $34\% \pm 11\%$ ) using both  $^{123}\text{I}$ -IPPA and rest-redistribution  $^{201}\text{Tl}$  imaging. A greater number of reversible defects were seen with  $^{123}\text{I}$ -IPPA than  $^{201}\text{Tl}$ . Patients who showed improvement in EF after revascularization had a greater number of reversible  $^{123}\text{I}$ -IPPA perfusion defects preprocedure compared with patients who showed no improvement in EF.

#### Myocardial Kinetics of $^{123}\text{I}$ -IPPA when Administered After Reperfusion Following Acute Myocardial Infarction

In this model of reperfused infarcted myocardium, we found no difference in  $^{123}\text{I}$ -IPPA uptake between infarcted and normal myocardium. In the most severely damaged regions where flow was reduced to 0%–10% of normal,  $^{123}\text{I}$ -IPPA activity after 2 h of restored flow, as determined by well counting, was relatively high at 64% of normal. In a similar study but with less severe myocardial injury, Rellas et al. (14) injected  $^{123}\text{I}$ -IPPA in dogs 90–120 min after reperfusion following a 90-min total LAD occlusion. By quantitative tomographic imaging, these investigators found initial  $^{123}\text{I}$ -IPPA uptake in infarcted regions equal to 72.5% of maximal activity in the same slice. The mechanism for the higher than expected amount of  $^{123}\text{I}$ -IPPA uptake in areas of severe myocyte injury may be due to the formation of

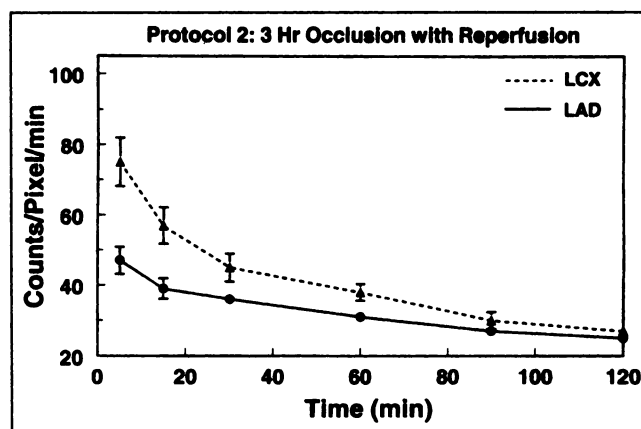


**FIGURE 6.** Time-activity curves from ROIs drawn on serial  $^{123}\text{I}$ -IPPA images of protocol 2 dogs. There was rapid, early-phase clearance of  $^{123}\text{I}$ -IPPA in normal LCX zone with slower clearance from reperfused LAD zone, suggesting ongoing impairment of fatty acid metabolism in reperfused zone.

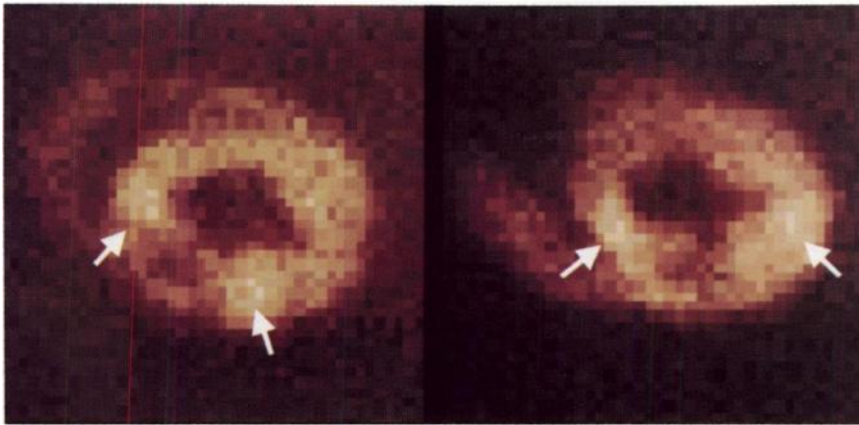


**FIGURE 7.** Representative ex vivo images from two protocol 2 dogs show enhanced  $^{123}\text{I}$ -IPPA uptake ("hot spots" indicated by white arrows) in perinecrotic border zone regions of myocardial risk area.

intracellular "soaps" resulting from precipitation of the fatty acid with excess calcium in the reperfused region or merely more rapid washout of  $^{123}\text{I}$ -IPPA from normal compared with infarct zone, yielding a relatively "normal" perfusion pattern several hours after tracer injection.

Rellas et al. (14) also found reduced clearance of  $^{123}\text{I}$ -IPPA from the reperfused infarct and peri-infarct regions on serial tomograms. The mechanism of this heterogeneity in  $^{123}\text{I}$ -IPPA clearance is unclear. It may be that the myocardium in the reperfused region is using substrates other than fatty acids for oxidative metabolism, or that the remote myocardium is metabolizing fatty acids at a high rate because of increased metabolic demands. This finding is supported by the experimental studies by Schwaiger et al. (15), demonstrating reduced  $^{11}\text{C}$ -palmitate clearance and increased FDG localization in a canine model of coronary occlusion and reperfusion. In this study, we found that very early after

$^{123}\text{I}$ -IPPA injection there was a brief period of relatively rapid tracer clearance in the reperfused region. This rapid clearance likely resulted from increased backdiffusion of the nonmetabolized tracer from myocytes that were irreversibly injured during the occlusion and early reperfusion periods. Fox et al. (16) have reported a considerable degree of back diffusion of  $^{11}\text{C}$ -palmitate (41%–49%) in canine myocardium with both ischemia and hypoxia.

#### CLINICAL IMPLICATIONS

Serial  $^{123}\text{I}$ -IPPA imaging at rest is under investigation for its use in assessing myocardial viability in patients with chronic CAD and LV dysfunction. Quantitative assessment of  $^{123}\text{I}$ -IPPA uptake and clearance on images acquired 4, 12, 20, 28 and 36 min after tracer administration can differentiate viable from nonviable myocardium and predict improvement in LV function after revascularization in patients with chronic ischemic heart disease (17–23). In a phase I/II study comprising 35 patients,  $^{123}\text{I}$ -IPPA uptake of >50% of maximal counts on initial images was a good predictor of left ventricular ejection fraction (LVEF) after revascularization (6). Iskandrian et al. (6) compared serial rest  $^{123}\text{I}$ -IPPA imaging with rest-redistribution  $^{201}\text{Tl}$  imaging in 21 patients with a mean LVEF of  $34\% \pm 11\%$ . There was high agreement between  $^{123}\text{I}$ -IPPA and  $^{201}\text{Tl}$  for presence or absence and nature (reversible, mild fixed, severe fixed) of perfusion defects, although there were more reversible  $^{123}\text{I}$ -IPPA defects than reversible  $^{201}\text{Tl}$  defects per patient. Furthermore, these investigators found that the number of reversible  $^{123}\text{I}$ -IPPA defects was greater in patients who had an improvement in LVEF after revascularization than in patients without an improvement. The experimental data in this study provide validating  $^{123}\text{I}$ -IPPA kinetic data for using serial  $^{123}\text{I}$ -IPPA imaging for detection of hibernating myocardium. We found substantial "rest redistribution" of  $^{123}\text{I}$ -IPPA in a canine model of sustained low flow, which was significantly greater than the amount of  $^{201}\text{Tl}$  redistribution in the same animals (Fig. 4). As expected, the mechanism of redistribution was differential  $^{123}\text{I}$ -IPPA washout between normal and hypoperfused myocardium.

In contrast,  $^{123}\text{I}$ -IPPA imaging after reperfusion in acute

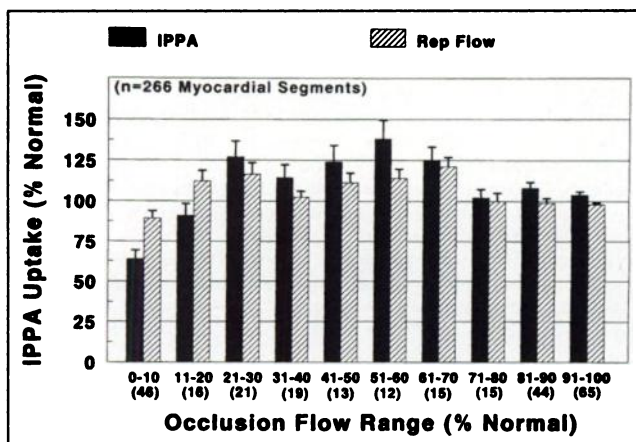


**FIGURE 8.** Mean IPPA activities (black bars) and injection flows (striped bars) from myocardial segments expressed as percentage of activity or flow in normal zone. Segments were grouped according to their flow reduction during occlusion period. Number of segments within each range is shown in parentheses below range label. Note that there was substantial IPPA uptake (64% of normal zone) in segments with  $\leq 10\%$  normal flow during occlusion. Also note that in peri-infarct, border zone regions (i.e., 21%–60% normal flow during occlusion),  $^{123}\text{I}$ -IPPA activity exceeded both injection flow and normal zone activity. Rep = reperfusion flow at time of  $^{123}\text{I}$ -IPPA injection.

myocardial infarction may not be useful for determination of myocardial salvage soon after reperfusion, as suggested from the experimental findings in protocol 2 in this study. Uptake of the tracer after reperfusion, preceded by 3 h of occlusion, was more reflective of reperfusion flow than residual viability (infarct size). Acutal hot spots of increased  $^{123}\text{I}$ -IPPA uptake were observed in the reperfused LAD region on ex vivo images of heart slices. This is reminiscent of the hot spots seen with  $^{99\text{m}}\text{Tc}$ -pyrophosphate imaging after acute infarction (24). Thus, a limitation of  $^{123}\text{I}$ -IPPA imaging for assessment of viability may be the identification of viable myocardium in patients with acute infarction. Further clinical trials appear warranted for determining the usefulness of  $^{123}\text{I}$ -IPPA for distinguishing viable from irreversibly injured myocardium in comparison with currently used radionuclide imaging techniques, such as rest-redistribution  $^{201}\text{Tl}$  imaging, FDG PET imaging and FDG SPECT imaging, using both recovery of function after revascularization and outcome endpoints, such as death and recurrent infarction during follow-up. The technique looks somewhat promising for identifying myocardial viability in chronic ischemic cardiomyopathy, but not in the setting of acute myocardial infarction.

#### ACKNOWLEDGMENTS

Supported by a research grant from Medco Research, Inc., Research Triangle Park, NC. Dr. Calnon's fellowship was funded by American Heart Association, Virginia affiliate.

#### REFERENCES

- Sobel BE, Weiss WES, Welch MJ, Siegel BA, Ter-Pogossian MM. Detection of remote myocardial infarction in patients with positron emission transaxial tomography and intravenous  $1\text{-}^{11}\text{C}$ -palmitate. *Circulation*. 1977;55:853-857.
- Ter-Pogossian MM, Klein MS, Markham J, Roberts S, Sobel BE. Regional assessment of myocardial metabolic integrity in vivo by positron emission tomography with  $1\text{-}^{11}\text{C}$ -palmitate. *Circulation*. 1980;61:242-254.
- Machulla HJ, Marsmann M, Dutschka K. Biochemical concept and synthesis of a radioiodinated phenyl fatty acid for in vivo metabolic studies of the myocardium. *Eur J Nucl Med*. 1980;5:171-173.
- Reske SN, Machulla HJ, Winkler C. Metabolism of 15-p-( $^{123}\text{I}$ -phenyl)-pentadecanoic acid in hearts of rats. *J Nucl Med*. 1982;23:10-18.
- Reske SN, Sauer W, Machulla HJ, et al. 15-(p( $^{123}\text{I}$ )-iodophenyl)-pentadecanoic acid as a tracer of lipid metabolism: comparison with ( $1\text{-}^{14}\text{C}$ ) palmitic acid in murine tissues. *J Nucl Med*. 1984;25:1335-1342.
- Iskandrian AS, Powers J, Cave V, Wasserleben V, Cassell D, Heo J. Assessment of myocardial viability by dynamic tomographic  $^{123}\text{I}$  iodopenylpentadecanoic acid imaging: comparison with rest-redistribution thallium 201 imaging. *J Nucl Cardiol*. 1995;2:101-109.
- Smith WH, Watson DD. Technical aspects of myocardial planar imaging with technetium-99m-sestamibi. *Am J Cardiol*. 1990;66:16E-22E.
- Heymann MA, Payne BD, Hoffman JIE, Rudolph AM. Blood flow measurements with radionuclide-labeled particles. *Prog Cardiovasc Dis*. 1977;20:55-79.
- Visser FC, van Eenige MJ, Westera G, et al. Metabolic fate of radioiodinated heptadecanoic acid in the normal canine heart. *Circulation*. 1985;72:565-571.
- Schön HR, Schelbert HR, Robinson GD, et al. C-11-labeled palmitic acid for the noninvasive evaluation of regional myocardial fatty acid metabolism with positron computed tomography I. Kinetics of C-11 palmitic acid in normal myocardium. *Am Heart J*. 1982;103:532-547.
- Reske SN, Sauer W, Machulla HJ, Winkler C. 15-(p( $^{123}\text{I}$ )-iodophenyl)-pentadecanoic acid as tracer of lipid metabolism: comparison with [ $1\text{-}^{14}\text{C}$ ]palmitic acid in murine tissues. *J Nucl Med*. 1984;25:1335-1342.
- Sansoy V, Glover DK, Watson DD, et al. Comparison of thallium-201 resting redistribution with technetium-99m-sestamibi uptake and functional response to dobutamine for assessment of myocardial viability. *Circulation*. 1995;92:994-1004.
- Koplan BA, Beller GA, Ruiz M, Yang JY, Watson DD, Glover DK. Comparison between thallium-201 and technetium-99m-tetrofosmin uptake with sustained low flow and profound systolic dysfunction. *J Nucl Med*. 1996;37:1398-1402.
- Rellas JS, Corbett JR, Kulkarni P, et al. Iodine-123 phenylpentadecanoic acid: detection of acute myocardial infarction and injury in dogs using an iodinated fatty acid and single-photon emission tomography. *Am J Cardiol*. 1983;52:1326-1332.
- Schwaiger M, Schelbert HR, Ellison D, et al. Sustained regional abnormalities in cardiac metabolism after transient ischemia in the chronic dog model. *J Am Coll Cardiol*. 1985;6:336-347.
- Fox KAA, Abendschein DR, Ambos HD, Sobel BE, Bergmann SR. Efflux of metabolized and nonmetabolized fatty acid from canine myocardium: implications for quantifying myocardial metabolism tomographically. *Circ Res*. 1985;57:232-243.
- Corbett J. Clinical experience with iodine-123-iodophenylpentadecanoic acid. *J Nucl Med*. 1994;35(suppl):32S-37S.
- Hansen CL. Preliminary report of an ongoing phase I/II dose range, safety, and efficacy study of iodine-123-phenylpentadecanoic acid for the identification of viable myocardium. *J Nucl Med*. 1994;35(suppl):38S-42S.
- Hansen CL, Heo J, Iskandrian AS. Prediction of improvement of left ventricular function after coronary revascularization from alterations in myocardial metabolic activity detected with I-123-phenylpentadecanoic acid dynamic SPECT imaging [abstract]. *J Am Coll Cardiol*. 1994;23:344A.
- Murray GL, Schad NC, Magill HL, Vander Zwaag R. Myocardial viability assessment with dynamic low-dose iodine-123-iodophenylpentadecanoic acid metabolic imaging: comparison with myocardial biopsy and reinjection SPECT thallium after myocardial infarction. *J Nucl Med*. 1994;35(suppl):43S-48S.
- Powers J, Cave V, Wasserleben V, Cassell D, Heo J, Iskandrian AS. Mechanisms and implications of redistribution during dynamic rest SPECT I-123 IPPA imaging [abstract]. *J Am Coll Cardiol*. 1994;23:423A.
- Tamaki N, Kawamoto M. The use of iodinated free fatty acids for assessing fatty acid metabolism. *J Nucl Cardiol*. 1994;1:S72-S78.
- Hansen CL, Heo J, Oliner C, Van Decker W, Iskandrian AS. Prediction of improvement in left ventricular function with iodine-123-IPPA after coronary revascularization. *J Nucl Med*. 1995;36:1987-1993.
- Willerson JT, Parkey RW, Maximilian BL, Bonte FJ. Technetium-99m stannous pyrophosphate "hot spot" imaging to detect acute myocardial infarcts. *Cardiovasc Clin*. 1979;10:139-148.